Final Design Report

Micromouse Sensing Subsystem

Prepared by:
Safiya Mia

Prepared for:
EEE3088F
Department of Electrical Engineering
University of Cape Town

May 17, 2024

Declaration

1. I know that plagiarism is wrong. Plagiarism is to use another's work and pretend that it is one's own.
2. I have used the IEEE convention for citation and referencing. Each contribution to, and quotation in, this report from the work(s) of other people has been attributed, and has been cited and referenced.
3. This report is my own work.
4. I have not allowed, and will not allow, anyone to copy my work with the intention of passing it off as their own work or part thereof.

May 17, 2024

Name Surname

Date

Contents

Chapter 1

Introduction

1.1 Problem Description

A micromouse is a compact robot equipped with wheels and sensors, designed to compete in a maze-solving contest. The micromouse must autonomously solve the maze without external assistance, and do this as fast as possible.

The robot consists of four primary subassemblies: the motherboard, processor, power circuit, and sensor module. The motherboard serves as the central hub, connecting all the subassemblies. The processor is responsible for executing all logical and computational tasks. The power circuit manages the distribution of power from the battery to the various subsystems. The sensor module, which includes the sensors and their associated circuitry, is crucial for wall detection.

To successfully navigate the maze, the micromouse must determine its position relative to the walls. It must identify if there is a wall directly in front, to the left, or to the right of it, as it cannot proceed forward if obstructed. The sensor subsystem independently collects this information and transmits it to the microcontroller, which then utilises the data to devise a path through the maze.

1.2 Scope and Limitations

The sensing subsystem development task involves designing a sensor PCB that acts as the micromouse's 'eyes.' Its main goal is to provide the microcontroller with real-time data to detect walls obstructing the micromouse's path, both in front and on the sides. This task includes selecting suitable sensors, implementing the necessary circuitry, and integrating the PCB with the system architecture.

The project is constrained by the size and weight of the sensor PCB to ensure it fits the micromouse design. Limitations in sensor range and accuracy may affect detection capabilities. Tight deadlines restrict the time available for design and testing, potentially impacting the quality and optimization of the subsystem. Additionally, budget constraints limit the selection of high-end sensors and components, which could affect overall efficiency.

1.3 GitHub Link

https://github.com/Imaanshaik/EEE3088F-Group-21-Project

Chapter 2

Requirements Analysis

2.1 Requirements

The requirements for a micromouse sensing module are described in Table 2.1.

Table 2.1: Requirements of the Sensing Subsystem.

Requirement ID	Description
R01	The sensing subsystem must be able to detect proximity to walls in front, to the left, and to the right of the micromouse.
R02	The sensing subsystem needs to physically integrate with the micromouse motherboard using the provided pin headers.
R03	The sensing subsystem should be capable of switching to a low power consumption mode, to prolong the battery life.
R04	The system must be able to mitigate the effects of ambient light on its overall performance.

2.2 Specifications

The specifications, refined from the requirements in Table 2.1, for the micromouse sensing module are described in Table 2.2.

Table 2.2: Specifications of the sensing subsystem derived from the requirements in Table 2.1.

Specification ID	Description
SP01	The sensing subsystem should output 3 analogue voltage signals (front, left, and right), each ranging from 0V to 3.3V which can be interpreted as a particular distance from a wall.
SP02	The sensing subsystem must link to the motherboard through a 2x14 pin connector block.
SP03	A LiPo 800mAh 3.7V battery must power the sensing subsystem. The current drawn must not be greater than 300mA at any time instance.
SP04	In 'power saving mode', the battery must draw less than 30mA of current.

2.3 Testing Procedures

A summary of the testing procedures detailed in chapter 4 is given in Table 2.3.

SP05	Different natural lighting conditions must not affect the outputs of the sensors.
SP06	The system must display the presence of a wall in front, to the right and/or to the left of the microcontroller using 3 LEDs on the processor board.

Table 2.3: Summary of Testing Procedures

Acceptance Test ID	**Description**
AT01	LED circuit powers on
AT02	Infrared sensor is able to detect light from adjacent LED
AT03	Sensing PCB fits onto motherboard
AT04	Power saving capability
AT05	Low current mode exists
AT06	System is robust through different natural lighting conditions
AT07	System is interfaced to the STM32F0 to produce LED outputs

2.4 Traceability Analysis

The show how the requirements, specifications and testing procedures all link, Table 2.4 is provided.

Table 2.4: Requirements Traceability Matrix

#	Requirements	Specifications	Acceptance Test
1	R01	SP01, SP06	AT01, AT02, AT07
2	R02	SP02	AT03
3	R03	SP03, SP04	AT04, AT05
4	R04	SP05	AT06

2.4.1 Traceability Analysis 1

R01 stipulates that the sensing subsystem must be able to detect proximity to walls in front and to the sides of the micromouse. From this, SP01 is derived, because it defines that the sensing subsystem should output 3 analogue voltage signals (front, left, and right), each ranging from 0V to 3.3V which can be interpreted as a particular distance from a wall. Furthermore, SP06 can also be derived. This is due to the fact that for R01 to be fulfilled, the micromouse needs a visual signal that it is detecting a wall as it traverses the maze. AT01 and AT02 are suggested because they verify SP01 - that the sensors are able to detect proximity, and AT07 is suggested because it verifies SP06.

2.4.2 Traceability Analysis 2

From R02, which states that the sensing subsystem needs to physically integrate with the micromouse motherboard using the provided pin headers, SP02 can be derived because it describes the specific headers the sensing subsystem will require to link to the motherboard - this is a 2x14 pin connector block. These can be tested through AT03 which tests that the micromouse and sensing board are physically compatible.

2.4.3 Traceability Analysis 3

R03, requires that sensing subsystem should be capable of switching to a low power consumption mode, to prolong the battery life. From this, SP03 and SP04 are derived, as they both detail ways in which the battery life will be prolonged by the system's design. AT04 and AT05 will verify the functionality of this power saving requirement and corresponding specifications.

2.4.4 Traceability Analysis 4

From R04, which requires that the system diminishes the effects of ambient light on its overall performance, SP05 can be derived. This is because SP05 specifies system robustness, that the sensing system output must not change under various natural lighting conditions. AT06 is designed to prove the fulfilment of R04 and SP05.

Chapter 3

Subsystem Design

3.1 Design Decisions

3.1.1 Final Design

To ensure that all potential performance and environmental factors were considered, different types of contactless sensors required comparison in order to select the most efficient and suitable one for the micromouse's sensing subsystem.

Table 3.1: Comparing Types of Contactless Sensors

Type	**Characteristics**
Infrared Light Detection	• Response Time: Fast • Size: Compact • Sensitivity: High • Cost: Low
Ultrasonic Sensor	• Response Time: Moderate to Fast • Size: Moderate to Large • Sensitivity: Moderate • Cost: Moderate
Laser Range Finder	• Response Time: Fast • Size: Moderate to Large • Sensitivity: High • Cost: High

From the information noted in **??**, the decision to use IR Light Detection was made. The combination of fast response time, compact size, high sensitivity, and low cost makes infrared sensors the perfect choice for a micromouse to detect walls and navigate through a maze, aligning with the requirements and specifications of the system.

Component Selection

To select the most adept IR sensor model for the micromouse, which must detect precise distances, have quick response times and a high sensitivity, the peak wavelength, dark current, and light current of different models need to be reviewed.

Table 3.2: Comparing Different IR Sensor Models

Parameter	BPW41N	MHL590PD12BHT	PD333-3B
Wavelength	950nm	920nm	940nm
Reverse Light Current	43 μA	30 μA	35 μA
Reverse Dark Current	2nA	5nA	5nA

[1]

After comparing a range of photodiodes from the JCLPCB, shown in 3.2, BPW41N was selected due to its high reverse light current and low reverse dark current. Furthermore, its wavelength of peak sensitivity is high, and corresponds to the peak wavelength of the selected IR LED - for optimal absorption.

To select the most suitable IR LED for the micromouse, which ensures optimal illumination and compatibility, the peak wavelength, radiant intensity and maximum forward current must be assed.

Table 3.3: Comparing Different IR LED Models

Parameter	SFH4544	IR423C	IR928-6C-F
Max Forward Current	100mA	100mA	50mA
Radiant Intensity	550mW/sr	11mW/sr	not specified
Peak Wavelength	950nm	940nm	940nm

[2]

After considering multiple options for an Infrared Emitter, it was concluded that SFH4544 would be the most suitable choice, given its very high radiant intensity and high current rating.

- Realising the need for a switching mechanism in the LED circuit to save power, a comparison between BJT and MOSFET was required for the sensing subsystem. It was concluded that a BJT is more appropriate than a MOSFET due to its precise current control and fast switching speeds, and because this is a low-current application. Furthermore, BJTs are cheaper than MOSFETs and component selection was limited by a strict budget.

The selection of the remaining circuit components was made with the following considerations:

- The gain and base-emitter voltage of the BJT will be used to bias the current through each LED.
- The typical operating voltage range of the op-amp must allow it to be powered by 3.3V.
- The selected resistors should have low tolerance to ensure that their actual values will be very close to the assumed ideal value used in calculations.

Table 3.4: Selection of other circuit components and their relevant parameters

Part Number	Component Type	Notable Parameters
MMBT2222A	Transistor (NPN)	• DC Current Gain at $I_c = 90\,\text{V}$: $h_{FE} \approx 240$ • Emitter Base Voltage: $V_{BE} \approx 0.7\,\text{V}$
LMV321IDBVR	Operational Amplifier	• Typical Operating Voltage: 2.7V – 5.5V
0805W8F6801T5E	6.8kΩ Resistor	• Tolerance: ±1%
0805W8F1004T5E	1MΩ Resistor	• Tolerance: ±1%

Designing the IR Emitter Circuit

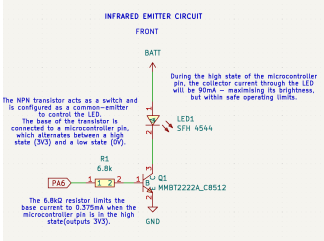

Figure 3.1: Infrared Light-Emitting Circuit

From 3.3, it was noted that the maximum forward current the selected LED model can handle is 100mA. Higher current increases brightness, but exceeding the max current risks damage to component. Thus, a current of 90mA was chosen to run through each LED. The following calculations show the process and result of the value of resistor R1 calculation.

$$I_{R1} = \frac{I_{\text{LED1}}}{h_{FE}} = \frac{90mA}{240} = 0.375\,\text{mA} \tag{3.1}$$

$$R1 = \frac{V_{\text{cc}} - V_{\text{BE}}}{I_{R1}} = \frac{3.3\,\text{V} - 0.7\,\text{V}}{0.375\,\text{mA}} = 6.933\,\text{k}\Omega \;\approx 6.8\,\text{k}\Omega\ \text{(E12 Value)}. \tag{3.2}$$

- The effect of using a slightly smaller E12 resistor value in this scenario, is that the base current of the transistor will be slightly larger than 0.375mA, resulting in a collector current that is marginally larger than the desired 90mA. This increase is still within safe operating limits of the LED model.

Designing the IR Sensor Circuit

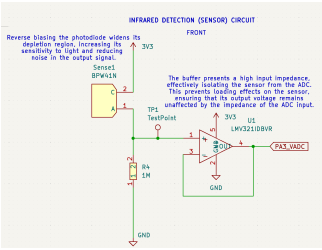

Figure 3.2: IR Detection and ADC Input Circuit

A large value of $1M\Omega$ is chosen for the resistor in series with the photodiode, so that the entire regulated voltage of 3.3V is not dropped across the sensor, preventing it from permanently reading 0V (GND). This minimises signal distortion.

Designing the Sensing Subsystem Layout

The subsystem contains 3 distinct IR Emitter Circuits and 3 IR Detector Circuits. Each IR Emitter Circuit is paired with a IR Detector Circuit and strategically positioned on a particular edge of the rectangular PCB board (which is situated at the front of the microcontroller). One pair is placed in front of the board, with another pair on the left side and the last pair pair on the right side of the board.

Each LED is bent horizontally, such that it will emit toward a potential wall directly in front of it. In this configuration, potential obstacles on the front, right, and left side of the micromouse are optimally covered. Similarly, each photodiode sensor is placed adjacent to its corresponding LED, directly facing the wall. This arrangement ensures thorough detection capability, as all possible orientations of possible maze walls are covered.

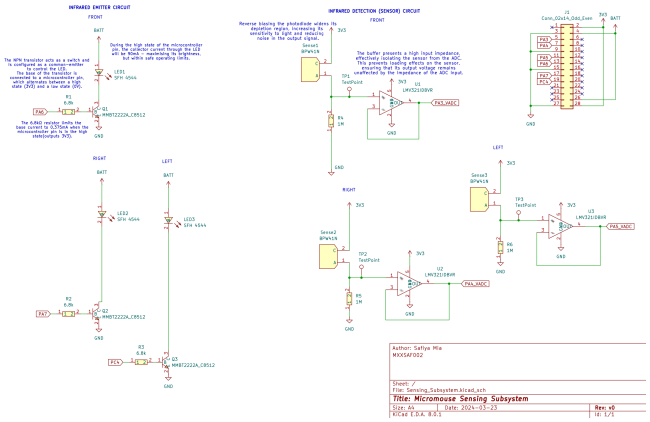

Figure 3.3: Schematic

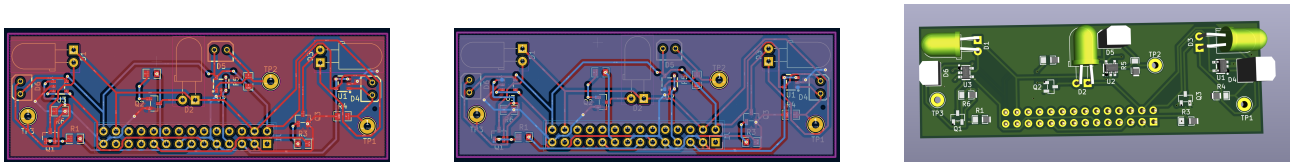

(a) Front PCB (b) Back PCB (c) 3D PCB

Figure 3.4: PCB

3.2 Failure Management

Table 3.5: Failure Management Strategies in PCB Design

Strategy Name	Description
Op-amp Buffer Failure Testing	Testpoints placed at each sensor output to gauge signal distortion and be compared to the ADC output; if op-amp configuration doesn't work as anticipated, remove the op amp and carefully solder a wire to connect the test point and appropriate pin.
General Component Failure	SMD resistors, transistors, and op-amps are used, and they can be removed simply by using two soldering irons with the component between the tips, like tweezers; through-hole components like LEDs and photodiodes can be desoldered and replaced if faulty. Resistors are spaced away from traces to avoid damage during desoldering process. SMD resistors can be replaced from Brendan's stock in White Lab.

3.3 System Integration and Interfacing

To interface the sensing subsystem with the microcontroller, the 2x14 pin header on the processing board is integrated with the corresponding connection on the sensor PCB.

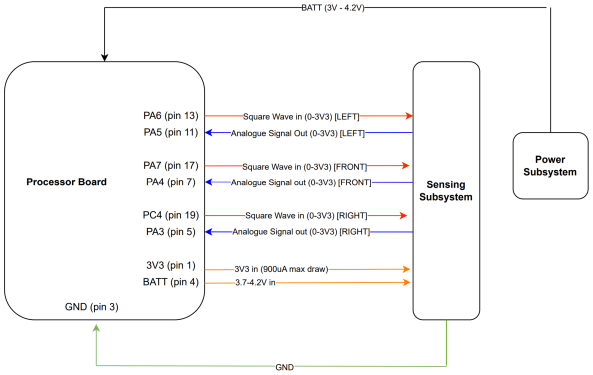

Figure 3.5: High-level System Interfacing Diagram

Table 3.6: Interfacing specifications

Interface	Description	Pins/Output
I001	The battery controls the collector voltage in each common-emitter configuration of the BJTs.	• BATT (pin 4) (3.7-4.2V) -> anode of LED1, LED2 and LED3
I002	The microcontroller's analogue pins are used to switch the state of the LEDs by changing the alternating the voltage delivered to the base of the transistor.	• PA6 (pin 13) (square wave with states 0V and 3.3V)-> base of left IR emitter circuit BJT • PA7 (pin 17) (square wave with states 0V and 3.3V) -> base of front IR emitter circuit BJT • PC4 (pin 19) (square wave with states 0V and 3.3V) -> base of 'left' IR emitter circuit BJT
I003	Regulated power delivered to each photodiode.	• 3V3 (pin 2) -> cathode of SENSE1, SENSE2 and SENSE3
I004	The buffered sensor output is inputted into 3 analogue pins	• PA3 (pin 5) (analogue signal between 0V and 3.3V) <- pin 4 of U1 • PA4 (pin 7) (analogue signal between 0V and 3.3V) <- pin 4 of U2 • PC5 (pin 11) (analogue signal between 0V and 3.3V) <- pin 4 of U3
I005	Op-amp power rail supply is connected to the regulated voltage and ground pin	• 3V3 (pin 2) -> pin 2 of U1, U2 and U3 • GND (pin 27) -> pin 5 of U1, U2 and U3

Chapter 4

Acceptance Testing

4.1 Tests

Table 4.1: Subsystem acceptance tests

Test ID	Description	Testing Procedure	Pass/Fail Criteria
AT01	LED circuit powers on	Simulate the battery voltage range (3.7V-4.2V) on a digital power supply and apply it to pin 4 of the sensing PCB. Use the other channel to apply 3.3V to the pin connected to the transistor base of the specific LED for testing. Monitor the current drawn by reading the display on the power supply. Repeat for each LED.	Pass: The displayed current has a margin of error of $\pm 8\%$ relative to 90 mA. Fail: The displayed current deviates by $>8\%$ from 90 mA.
AT02	Infrared sensor detects light from adjacent LED	Replicate the connections required for AT01. Add a connection between the 3.3V supply and pin 1 of the sensing board. Connect a multimeter to the output of the adjacent sensor. Place a reflective obstacle in front of the LED and move it (up to 20cm) while monitoring the output voltage. Repeat for each LED-sensor pair.	Pass: Voltage increases by >1V when the obstacle is closest to the LED compared to when it's farther away. Fail: Voltage change <1V is observed.
AT03	Sensing PCB fits onto motherboard	Align the 2x14 male connectors on the sensing board to the 2x14 female connectors on the motherboard and click into place.	Pass: The boards click into place without damaging the connectors. Fail: The sensing board cannot connect, or pins bend/break.

AT04	Power saving capability	Set the DC power supply channels to 3.3V and 3.7V and connect these to respective sensing PCB pins. Use a signal generator to apply a square wave (0-3.3V) to the transistor base pin of the LED under examination. Connect the output pin of the sensor to an oscilloscope and observe the waveform. Repeat for all 3 LED-sensor pairs.	Pass: Output is a distinct square wave with a high state (non-zero value below 3.3V) and a low state (0V). Fail: Output waveform is not a discernible square wave with a high state (non-zero value below 3.3V) and a low state (0V).
AT05	Low current mode exists	Duplicate the pin 1 and pin 4 connections from AT04. Connect all 3 transistor base pins to an infinitesimal (zero) voltage, simulating the 'low' state. Monitor the current drawn by the 3.7V battery on the DC power supply screen.	Pass: The total current drawn is <30mA. Fail: The total current drawn is >30mA.
AT06	System is robust through different natural lighting conditions	Set up the sensing system in a lab environment. Connect the sensor outputs to a multimeter and observe the display. Place a desk lamp next to the sensing PCB and observe the voltage output. Place the subsystem next to a sunlit window and observe the output.	Pass: The output does not vary by more than ±5% across lighting conditions. Fail: The output varies by more than ±5%.
AT07	System is interfaced to the STM32F0 to produce LED outputs	Set up the sensing system following the interfacing diagram. Program the ADC to monitor sensor outputs and toggle PB7 (left), PB6 (front), and PB5 (right) to represent the presence of a wall. Repeat the procedure of moving the reflective material towards and away from the sensor, as in AT02, and observe PB7, PB6, and PB5.	Pass: LED outputs correctly correspond to sensor inputs. Fail: LED outputs do not correctly correspond to sensor inputs.

4.2 Critical Analysis of Testing

Table 4.2: Subsystem acceptance test results

Test ID	Description	Result
AT01	LED circuit powers on	Pass
AT02	Infrared sensor is able to detect light from adjacent LED	Pass
AT03	Sensing PCB fits onto motherboard	Pass
AT04	Power saving capability	Pass
AT05	Low current mode exists	Pass
AT06	System is robust through different natural lighting conditions	Pass
AT07	System is interfaced to the STM32F0 to produce LED outputs	Fail

4.2.1 AT01

The purpose of this test was to verify that the LEDs were switched on at optimal brightness, following the design in 3.1. After applying the testing procedure to the front LED, it was observed that the collector current through the front LED circuit was approximately 96mA. The test was repeated for both the left and right LED, yielding an identical current reading on the power supply screen. It was assessed that these LED circuits passed the test, because the pass/fail criteria of the acceptance test allows an 8% error margin from the ideal value of 90mA. This slightly high result can partially be attributed to the use of the lower E12 resistor values at the base of the transistors, as discussed in the design section. Another contributor could be the tolerance of the power supply machine and the uncertainty associated with its measurements. Furthermore, the current through the SFH4544 LED is still within the safe operating limit of 100mA, specified in its datasheet. The important result of this test was the knowledge that all 3 LED emitter circuits are definitely capable of emitting infrared light.

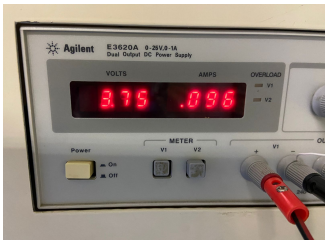

Figure 4.1: Collector current drawn from the battery with one LED turned on

4.2.2 AT02

Moving on to AT02, I sought to verify the functionality of the Infrared Detector Circuit, following the design in 3.2. After following the testing procedure, beginning with the front LED and sensor pair, the output voltage reading on the multimeter was strange and unexpected - it was fluctuating in the mV range, whether there was an obstacle in front of the LED-sensor pair or not. Because AT01 was passed, it meant that the problem was specifically located in the IR detector circuit, and not in the emitter

circuit. I started the debugging process by verifying the continuity of the circuit, comparing the board traces to my KiCad schematic. It was discovered that photodiode BPW41N photodiode was connected such that it was forward biased, instead of reverse biased, in the circuit configuration. I performed the diode test on the left and right LED, and discovered that they were similarly soldered incorrectly. This issue could be simply resolved, thanks to the failure management design of using through-hole sensors to populate my board. This procedure was applied - the sensors were de-soldered (with assistance from a friend), and soldered with the anode and cathode connected to the correct traces. A tutor informed me that even though my footprint showed the correct connection, a manufacturing misunderstanding occurred because the CPL file did not match the footprint.

After repeating AT02 on each LED, now with the correctly oriented photodiodes, a lovely result was observed on the multimeter screen. The figures below clearly depict that the sensors are functioning correctly - with significant voltage drop between the very close and far distance to the reflective wall material. Because this observed voltage drop was >1V for all 3 sensors tested, the sensing subsystem passed the test.

Figure 4.2: Sensor output when reflective obstacle is very close to sensor

Figure 4.3: Sensor output when reflective obstacle is near sensor

Figure 4.4: Sensor output when reflective obstacle is far (>20cm) from sensor

4.2.3 AT03

This was a relatively easy test to perform. The sensing PCB did not come populated with the appropriate headers as per instruction, but the process of collecting 2x14 male headers from the lab technician and soldering them carefully onto the board was quick and hassle-free. I was slightly careful of the traces I had running through my header, which I did not want to burn. After the soldering job was done, and I was satisfied with how the board clicked into the micromouse processor board headers, I evaluated a pass for this test.

4.2.4 AT04

To test that the sensing subsystem was capable of saving battery power, the testing procedure for AT04 was applied and the following results were observed.

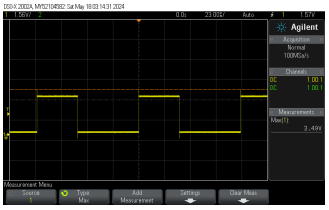

Figure 4.5: Square wave output to demonstrate power saving

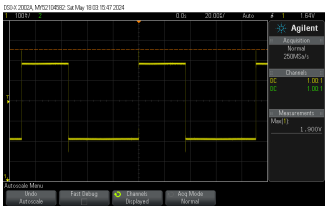

Figure 4.6: Square wave output to demonstrate power saving with different amplitude

It is clear that the sensing subsystem is still able to sense proximity to a wall, despite a changing input voltage. The low state voltage applied to the transistor inputs correspond to the zero voltage observed at the output. It is also noted that the duty cycle at the output corresponds to the duty cycle of the input waveform. This process was repeated for all sense direction circuits, and all three infrared emitter-detector circuit pairs passed the test.

4.2.5 AT07

This was the only test that failed, and it can primarily be attributed to poor time management: underestimating the time that rigorous testing takes, and visiting the lab during peak hours. I did not allocate sufficient time to complete the procedure for AT07.

Chapter 5

Conclusion

Despite the successful functionality of the sensing board in terms of accurate voltage signal outputs, power saving, robustness despite different lighting conditions, and seamless physical integration with the motherboard, its lack of interfacing capability with the microcontroller makes it ineffective for the micromouse application. The inability to communicate with the microcontroller prevents the subsystem from completing its intended purpose within the larger system architecture.

That being said, the successful completion of all other tests underscores the subsystem's potential to function in the desired manner. Its only missing link is the interface with the microcontroller, suggesting that it does not require discarding - it needs integration to fully unlock its capabilities.

Recommendations

In future, the need to focus on integrating the sensing board with the microcontroller has been understood. Additionally, refining testing methods for better efficiency and ensuring documentation aligns with manufacturing processes are practical steps for enhancing the subsystem performance and reliability. For example, to mitigate the photodiodes being soldered incorrectly, the CPL file and PCB footprint can be cross-referenced.

Bibliography

R